FORMATION OF THE TENSOR MESON $A_2(1320)$ IN PHOTON–PHOTON INTERACTIONS

PLUTO Collaboration

Ch. BERGER, A. DEUTER, H. GENZEL, W. LACKAS, J. PIELORZ [1], F. RAUPACH [2], W. WAGNER [3]
I. Physikalisches Institut der RWTH Aachen [4], Fed. Rep. Germany

A. KLOVNING, E. LILLESTÖL
University of Bergen [5], Norway

J. BÜRGER, L. CRIEGEE, F. FERRAROTTO [6], G. FRANKE, M. GASPERO [6], Ch. GERKE [7], G. KNIES, B. LEWENDEL, J. MEYER, U. MICHELSEN, K.H. PAPE, B. STELLA [6], U. TIMM, G.G. WINTER, M. ZACHARA [8], W. ZIMMERMANN
DESY, Hamburg, Fed. Rep. Germany

P.J. BUSSEY, S.L. CARTWRIGHT [9], J.B. DAINTON, B.T. KING, C. RAINE, J.M. SCARR, I.O. SKILLICORN, K.M. SMITH, J.C. THOMSON
University of Glasgow [10], UK

O. ACHTERBERG [11], V. BLOBEL, D. BURKART, K. DIEHLMANN, M. FEINDT, H. KAPITZA, B. KOPPITZ, M. KRÜGER [12], M. POPPE, H. SPITZER, R. van STAA
II. Institut für Experimentalphysik der Universität Hamburg [4], Fed. Rep. Germany

C.Y. CHANG, R.G. GLASSER, R.G. KELLOGG, S.J. MAXFIELD, R.O. POLVADO [13], B. SECHI-ZORN, J.A. SKARD, A. SKUJA, A.J. TYLKA, G.E. WELCH, G.T. ZORN
University of Maryland [14], USA

F. ALMEIDA [15], A. BÄCKER, F. BARREIRO, S. BRANDT, K. DERIKUM [16], C. GRUPEN, H.J. MEYER, H. MÜLLER, B. NEUMANN, M. ROST, K. STUPPERICH, G. ZECH
Universität-Gesamthochschule Siegen [4], Fed. Rep. Germany

G. ALEXANDER, G. BELLA, Y. GNAT, J. GRUNHAUS
Tel-Aviv University [17], Israel

and

H. JUNGE, K. KRASKI, C. MAXEINER, H. MAXEINER, H. MEYER and D. SCHMIDT
Universität-Gesamthochschule Wuppertal [4], Fed. Rep. Germany

[1] Deceased.
[2] Present address: Université de Paris Sud, Orsay, France.
[3] Present address: University of California at Davis, CA, USA.
[4] Supported by the BMFT, Fed. Rep. Germany.
[5] Partially supported by Norwegian Council for Science and Humanities.
[6] Rome University, partially supported by INFN, Sezione di Roma, Italy.
[7] Present address: CERN, Geneva, Switzerland.
[8] Institute of Nuclear Physics, Cracow, Poland.
[9] Present address: Rutherford Appleton Laboratory, Chilton, UK.
[10] Supported by the UK Science and Engineering Research Council.
[11] Present address: Texaco, Hamburg, Fed. Rep. Germany.
[12] Present address: Universität Karlsruhe, Fed. Rep. Germany.
[13] Present address: Northeastern University, Boston, MA, USA.
[14] Partially supported by the Department of Energy, USA.
[15] On leave of absence from Instituto de Fisica, Universidad Federal do Rio de Janeiro, Brazil.
[16] Present address: BESSY, Berlin, Fed. Rep. Germany.
[17] Partially supported by the Israeli Academy of Sciences and Humanities – Basic Research Foundation.

0370-2693/84/$03.00 © Elsevier Science Publishers B.V.
(North-Holland Physics Publishing Division)

Received 2 October 1984

We have measured the reaction $\gamma\gamma \to \pi^+\pi^-\pi^0$ using the PLUTO detector at PETRA. A pronounced enhancement is seen in the $\pi^+\pi^-\pi^0$ mass distribution corresponding to the A_2 meson. The event configuration in this enhancement favors a 2^+ spin–parity assignment. The value of $\Gamma_{\gamma\gamma} = 1.06 \pm 0.18 \pm 0.19$ keV obtained for the two-photon decay width of the A_2 agrees with previous measurements and with quark model predictions.

The formation of neutral tensor mesons in photon–photon reactions has been investigated recently [1] and their two-photon decay widths, $\Gamma_{\gamma\gamma}$, have been determined. These decay widths are of interest because the quark model predicts the following relations between the $\Gamma_{\gamma\gamma}$ of the three neutral tensor mesons and their mass values:

$$\frac{\Gamma_{\gamma\gamma}(A_2)}{m_A^3} : \frac{\Gamma_{\gamma\gamma}(f)}{m_f^3} : \frac{\Gamma_{\gamma\gamma}(f')}{m_{f'}^3} \tag{1}$$
$$= 3 : (\sin\vartheta + \sqrt{8}\cos\vartheta)^2 : (\sqrt{8}\sin\vartheta - \cos\vartheta)^2 ,$$

where ϑ is the mixing angle between the octet, f_8, and the singlet, f_1, states of flavor SU(3), such that

$$f' = f_8 \cos\vartheta - f_1 \sin\vartheta ,$$

$$f = f_8 \sin\vartheta + f_1 \cos\vartheta .$$

From relation (1) the following ϑ-independent relation can be derived:

$$3\Gamma_{\gamma\gamma}(A_2)/m_A^3 = \Gamma_{\gamma\gamma}(f)/m_f^3 + \Gamma_{\gamma\gamma}(f')/m_{f'}^3 . \tag{2}$$

The production of the A_2 meson in photon–photon collisions was first seen by the Crystal Ball detector [2] in the decay mode $A_2 \to \eta\pi^0$. The dominant decay mode, $A_2 \to \rho^\pm\pi^\mp$, which has been used by the CELLO [3] and JADE [4] collaborations, is also utilised here to measure $\Gamma_{\gamma\gamma}(A_2)$.

The data were taken by the PLUTO detector and correspond to an integrated luminosity of 41.5 pb^{-1} at an e^+e^- CM energy of 34.7 GeV. The PLUTO detector has been described elsewhere [5,6]. For the present analysis, the inner detector and the forward spectrometers were used to measure charged tracks, and the barrel, endcap and Large Angle Tagger (LAT) shower counters determined the photon energies and positions. The Small Angle Tagger (SAT) and the LAT shower counters were used as antitag devices to ensure that both interacting photons were almost real.

The data used here satisfied at least one of the following three main trigger conditions:

(1) Two tracks in the inner detector with transverse momenta larger than 350 MeV/c separated by an azimuthal angle larger than 94°.

(2) At least one track in each half of one of the forward spectrometers.

(3) Total energy of more than 4 GeV deposited in the LAT shower counters.

To obtain for analysis a sample of events of the type $\gamma\gamma \to \pi^+\pi^-\gamma\gamma$ we used the following off-line event selection:

(1) Each event was required to have two charged tracks with opposite charge and two showers not associated with the tracks. The minimum energy required for the showers was 100 MeV and 120 MeV for the barrel and LAT counters respectively. Showers measured in the endcap counters were accepted only if they were detected also by the endcap proportional chambers.

(2) To ensure that both interacting photons were quasi-real, an antitag condition was required, namely that no shower in the LAT or SAT had an energy greater than 6 GeV.

(3) To enrich the sample with fully reconstructable events and to obtain a low invariant mass squared, Q^2, for the interacting photons, we have used the fact that the total transverse momentum of the hadrons with respect to the beam line should be small. Denoting the total transverse momentum of the charged (neutral) particles by p_{Tc} (p_{Tn}), we then required

(a) $|p_{Tc} + p_{Tn}| < 350$ MeV/c.

(b) Angle between the two vectors p_{Tc} and $-p_{Tn}$ to be less than 0.35 radians.

The selected sample was then kinematically fitted to the channel $\gamma\gamma \to \pi^+\pi^-\pi^0$ in two steps. Firstly, the events were fitted in the transverse plane requiring

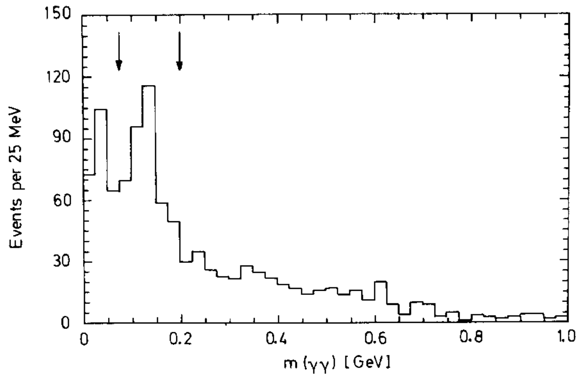

Fig. 1. Invariant mass of the two outgoing photons, $m(\gamma\gamma)$, for events after cuts and after a kinematic fit imposing transverse momentum conservation. The two arrows mark the π^0 mass range used in the analysis.

$p_{\mathrm{Tc}} + p_{\mathrm{Tn}} = 0$ (two-constraint fit). In fig. 1 the invariant mass of the two outgoing photons is shown for events which fitted with a χ^2 probability greater than 2%. An enhancement of events near the π^0 mass is seen. Secondly, the events in the π^0 region ($75 < m_{\gamma\gamma} < 200$ MeV) were fitted with the additional constraint of the $\gamma\gamma$ invariant mass being equal to the π^0 mass. In total, 294 events satisfied this three-constraint fit with a χ^2 probability larger than 2% and were accepted for physics analysis. From Monte Carlo studies we estimate that these events have very small Q^2 with an average value of $\sim 4 \times 10^{-4}$ GeV^2.

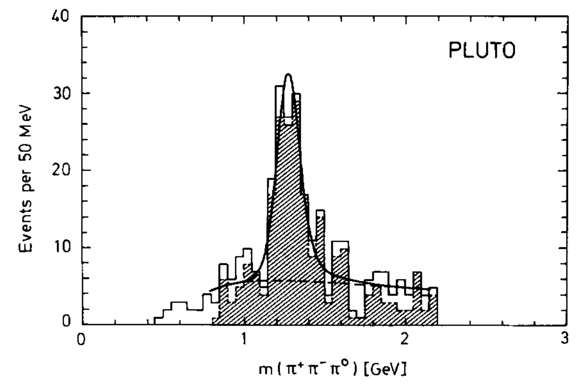

Fig. 2. Invariant mass of the three pions, $m(\pi^+\pi^-\pi^0)$, in the final event sample. The shaded area corresponds to a subsample of events with a $\pi^+\pi^0$ or $\pi^-\pi^0$ mass combination in the ρ mass band. The solid line represents the fit to the data and the dashed curve describes the background.

Fig. 2 shows the $\pi^+\pi^-\pi^0$ invariant mass ($\sqrt{s}$) distribution. A clear enhancement is seen at the A_2 mass. No signal is observed in the background events with $m(\gamma\gamma)$ outside the π^0 mass band. The event configuration in the A_2 enhancement is consistent with the expectation that the $\pi^+\pi^-\pi^0$ state is produced entirely via the $\rho\pi$ decay channel. This can be seen by comparing the enhancement with the shaded area in fig. 2 which corresponds to the sub-sample of events with a $\pi^+\pi^0$ or $\pi^-\pi^0$ mass combination in the ρ mass band of $m_\rho \pm 200$ MeV. The solid curve shown in fig. 2 is the result of a fit to an incoherent sum of a background term of the form $A/\sqrt{s} + B/s$ and a relativistic Breit–Wigner shape folded with the experimental mass resolution of 54 ± 10 MeV determined from Monte Carlo studies. The following energy dependent width was used in the Breit–Wigner expression

$$\Gamma_{\mathrm{A}}(s) = \Gamma_{\mathrm{A}}(m_{\mathrm{A}}^2)(p_\rho/p_\rho^0)^{2L+1} D_{\mathrm{L}}(p_\rho^0 r)/D_{\mathrm{L}}(p_\rho r) \,. \quad (3)$$

Here p_ρ^0 is the ρ momentum in the 3-π rest frame for 3-π invariant mass equal to the A_2 mass, m_{A}; p_ρ is the corresponding ρ momentum calculated for the 3-π invariant mass $\sqrt{s}$. D_{L} is the barrier penetration factor [7], with L being the orbital angular momentum (i.e. $L = 2$ for $A_2 \to \rho\pi$ decay), and r is the interaction range, which was set to 1 fm as in ref. [8].

A fit to the observed mass distribution with the free parameters m_{A} and Γ_{A} yielded the values: $m_{\mathrm{A}} = 1279 \pm 12$ MeV and $\Gamma_{\mathrm{A}} = 69^{+38}_{-31}$ MeV with 97 ± 18 events attributed to A_2 formation. Monte Carlo studies show that the effects of the detector and analysis procedure reduce the observed mass by ~15 MeV. Hence, our best values for the resonance mass and width are, $m_{\mathrm{A}} = 1294 \pm 12 \pm 11$ MeV, $\Gamma_{\mathrm{A}} = 69^{+38}_{-31} \pm 30$ MeV, where the systematic error in the mass value comes from the finite Monte Carlo statistics and the theoretical uncertainty in the interaction range, r. The systematic error quoted for Γ_{A} reflects our uncertainty in the experimental mass resolution. An acceptable fit is also obtained when m_{A} and Γ_{A} are fixed to the world average values [9] of $m_{\mathrm{A}} = 1318 \pm 5$ MeV, $\Gamma_{\mathrm{A}} = 110 \pm 5$ MeV.

To evaluate the two-photon decay width and to determine the helicity structure of the $A_2 \to \gamma\gamma$ coupling, we have simulated by the Monte Carlo method the reaction

$$e^+e^- \to e^+e^-\gamma\gamma\,, \quad \gamma\gamma \to \pi^+\pi^-\pi^0\,,$$

using for the luminosity function the standard formula given in ref. [10]. The Monte Carlo events were generated according to a differential cross section with constructive interference [11] between the $\rho^+\pi^-$ and the $\rho^-\pi^+$ decay terms:

$$d\sigma = 2\pi(2J+1)(m_A/s)\,\Gamma_{\gamma\gamma}/[(m_A^2-s)^2+m_A^2\Gamma_A^2]$$

$$\times \sum_\lambda R_{\lambda\lambda}\left|\frac{T_\lambda(A_2\to\rho^+\pi^-\to3\pi)}{m_\rho^2-s_\rho^+-im_\rho\Gamma_\rho^+}+\frac{T_\lambda(A_2\to\rho^-\pi^+\to3\pi)}{m_\rho^2-s_\rho^--im_\rho\Gamma_\rho^-}\right|^2 d(\mathrm{LIPS})_{3\pi}\,. \quad (4a)$$

Here $J(\lambda)$ is the A_2 spin (helicity), $d(\mathrm{LIPS})_{3\pi}$ is the three-pion Lorentz invariant phase space element, $s_\rho^\pm$ is the invariant mass of the $\pi^\pm\pi^0$ system, and $\Gamma_\rho^\pm$ is the energy dependent width of the $\rho^\pm$ according to eq. (3) with $L = 1$ and $r = 0.58$ fm [12]. The transition amplitude, $T_\lambda(A_2\to\rho\pi\to3\pi)$, is given by

$$T_\lambda(A_2\to\rho\pi\to3\pi) = 32\pi^2(m_A\Gamma_{\rho\pi}m_\rho\Gamma_\rho\sqrt{ss_\rho}/p_\rho p_\pi)^{1/2}$$

$$\times\sum_m C^{J\lambda}_{L,\lambda-m,1,m}\,Y_L^{\lambda-m}(\vartheta_\rho,\varphi_\rho)\,Y_1^m(\vartheta_\pi,\varphi_\pi), \quad (4b)$$

where p_ρ, ϑ_ρ and φ_ρ are the ρ meson momentum, polar and azimuthal angles measured in the A_2 rest frame; p_π, ϑ_π and φ_π are the corresponding variables of the π^0, measured in the ρ rest frame. All angles are determined with respect to the e^+e^- beam line which is the angular momentum quantization axis. The $A_2\to\rho\pi$ decay width, $\Gamma_{\rho\pi}$, depends on s and s_ρ following eq. (3). The spherical harmonic products in eq. (4b) are multiplied by the Clebsch–Gordan coefficients $C^{J\lambda}_{L,\lambda-m,1,m}$ with m being the third component of the ρ spin.

The density matrix elements, $R_{\lambda\lambda}$, give the relative contributions of different helicity states to the A_2 formation. Since the interacting photons are almost real, they do not couple to $\lambda = \pm1$. Furthermore one expects from theoretical arguments [13] that the helicities $|\lambda| = 2$ will dominate over $\lambda = 0$.

The Monte Carlo events were passed through a full detector simulation where particular care was given to the following effects:

(1) The trigger efficiency, which was calibrated from data events with topology similar to the final A_2 events and with redundant trigger conditions.

(2) The efficiency for photon recognition, which was evaluated for the central detector using Dalitz pairs, and for the forward spectrometer using photons radiated from Bhabha events.

For the spin–parity analysis we have chosen to study two distributions:

(1) The distribution of the three pions in their CM system, using the parameter Λ [14] of the Dalitz density triangle plot, defined as

$$\Lambda = |\boldsymbol{p}_{\pi+}\times\boldsymbol{p}_{\pi-}|^2/\max(|\boldsymbol{p}_{\pi+}\times\boldsymbol{p}_{\pi-}|^2)\,,$$

which varies between 0 and 1, corresponding to events at the boundary and center of the kinematically allowed region of the Dalitz triangle.

(2) The distribution of the polar angle α of the normal to the A_2 decay plane measured with respect to the beam line, which is a good approximation to the incoming $\gamma\gamma$ direction.

Fig. 3 shows distributions of these two quantities

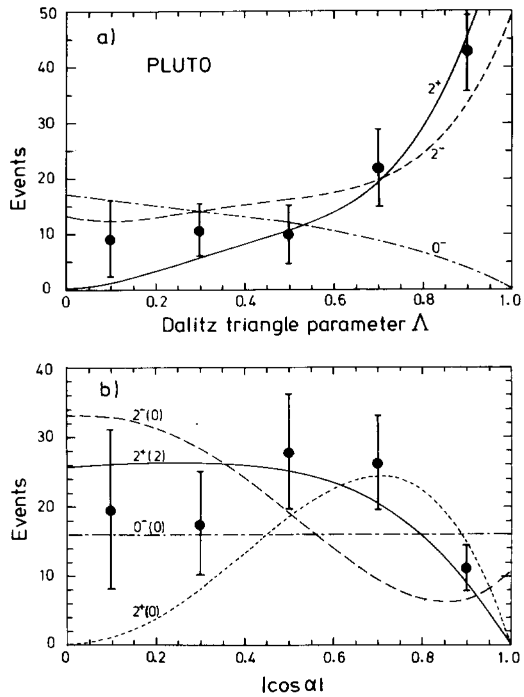

Fig. 3. Distributions of (a) Dalitz triangle parameter Λ (see text), (b) $|\cos\alpha|$, where α is the polar angle of the normal to the decay plane. The data are corrected for background and detector effects. The error bars include also systematic errors apart from an overall normalization uncertainty. The different curves correspond to various $J^P(\lambda)$ expectations.

for events with $1.15 \leqslant \sqrt{s} \leqslant 1.45$ GeV. The background contamination (on average 26%) in these distributions was estimated from the corresponding distributions of the side bands outside the A_2, and then subtracted bin by bin. The resulting distributions were then further corrected for detector and data analysis inefficiencies. The curves, normalized by the best fit to the data points, show the distributions for several spin–parity assignments for the observed enhancement. We compare the data in fig. 3 with all possible spin–parity assignments having $J \leqslant 2$, namely: $J^P = 2^+$ ($L = 2$) with $|\lambda| = 2$ and $\lambda = 0$; $J^P = 2^-$ ($L = 1$, neglecting a possible $L = 3$ contribution) with $\lambda = 0$; and $J^P = 0^-$ ($L = 0$). Note that a $J^P = 0^+$ resonance cannot decay into 3 pions, and $J^P = 1^\pm$ as well as $J^P = 2^-$ with $|\lambda| = 2$ are excluded by the Yang theorem [15].

The comparison of the data and predictions in fig. 3a clearly excludes the $J^P = 0^-$ assignment ($\chi^2/n_D = 33/4$). The data are in good agreement with the $J^P = 2^+$ assignment ($\chi^2/n_D = 2.4/4$) which is identical for $|\lambda| = 2$ and $\lambda = 0$. The data in fig. 3a are also consistent with $J^P = 2^-$, but this hypothesis is ruled out by the $|\cos\alpha|$ distribution in fig. 3b for which $\chi^2/n_D = 12.3/4$. From the same $|\cos\alpha|$ distribution the data are seen to be consistent within errors both with $J^P(\lambda) = 2^+(0)$, and $2^+(2)$ having $\chi^2/n_D = 6.8/4$ and 2.8/4 respectively. A fit to a linear combination of both helicity states yields a $|\lambda| = 2$ fraction of 62 ± 39%. This result is consistent with the preliminary JADE [4] results for the A_2 and with the theoretical expectations of $|\lambda| = 2$ dominance [13]. The same observation was also reported for $\gamma\gamma \to$ f production [2, 16].

To evaluate the $\gamma\gamma$ partial width, $\Gamma_{\gamma\gamma}$, of the A_2, we have determined the overall detector, trigger and data selection efficiency to be 0.61 ± 0.09%, for the 2^+ assignment and the helicity mixture found above. The 15% uncertainty associated with this efficiency is due to the limited Monte Carlo statistics (6%), uncertainties in the fraction of $\lambda = 0$ production (3%), trigger efficiency (6%), and detection efficiency for charged tracks (4%) and for photons (10%).

A correction was applied for event loss due to electronic noise simulating a photon. This was estimated by analysing two-track events with 3 photons and discarding the least energetic photon. From the mass distribution of these events we calculate the loss to be 11 ± 7.8%.

Prior to the final evaluation of $\Gamma_{\gamma\gamma}$, additional effects, not taken fully into account in the Monte Carlo simulation, must be considered in order to evaluate the systematic error:

(1) Uncertainty of 5% in the selection procedure. This was estimated by varying slightly the different selection cuts.

(2) Uncertainties in the invariant $\pi^+\pi^-\pi^0$ mass resolution and Breit–Wigner shape used for the resonance fit (7%).

(3) Errors in the integrated luminosity and $A_2 \to \rho\pi$ branching ratio (3% each).

Thus, the value obtained for the A_2 decay width into two photons is:

$$\Gamma_{\gamma\gamma} = 1.06 \pm 0.18 \pm 0.19 \text{ keV}.$$

The second quoted error is the combined systematic uncertainty of all the effects discussed above added in quadrature. If the A_2 mass and its total width are fixed to the world average values [9], we obtain a $\Gamma_{\gamma\gamma}$ of 1.16 ± 0.14 ± 0.21 keV, which is consistent with the above value.

Our value for $\Gamma_{\gamma\gamma}$ agrees within errors with those measured by the Crystal Ball [2] (0.77 ± 0.18 ± 0.27 keV), CELLO [3] (0.81 ± 0.19 ± 0.27 keV) and JADE [4] (0.84 ± 0.07 ± 0.15 keV). Using eq. (1) with a world average value $\Gamma_{\gamma\gamma}(\mathrm{f}) = 2.64 \pm 0.13$ keV [2,4,5,16,17] and a mixing angle $\vartheta = 27° \pm 3°$ [9], the quark model predicts $\Gamma_{\gamma\gamma}(A_2) = 0.99 \pm 0.05$ keV. The value of $\Gamma_{\gamma\gamma}(A_2)$ may also be predicted from relation (2) which is independent of the mixing angle. Using the value of $B(\mathrm{f}' \to K\bar{K})\,\Gamma_{\gamma\gamma}(\mathrm{f}') = 0.11 \pm 0.02 \pm 0.04$ keV measured by TASSO [18], and assuming $B(\mathrm{f}' \to K\bar{K}) = 1$, leads to $\Gamma_{\gamma\gamma}(A_2) = 1.00 \pm 0.05$ keV. Both predictions are in good agreement with our measured value.

In conclusion, we have observed A_2 formation in photon–photon interactions through its $\rho\pi$ decay channel. The event distribution in the Dalitz triangle plot and the decay plane angular distribution exclude $J^P = 0^-$, 2^- and agree with the $J^P = 2^+$ assignment in a dominant $|\lambda| = 2$ alignment. The decay width into two photons is measured to be $\Gamma_{\gamma\gamma} = 1.06 \pm 0.18 \pm 0.19$ keV, in agreement within errors both with previous measurements and quark model predictions.

We wish to thank the members of the DESY directorate for the hospitality extended to the university groups. We are indebted to the PETRA machine group and the DESY computer centre for their excellent performance during the experiment. We gratefully acknowledge the efforts of all the engineers and technicians who have participated in the construction and maintenance of the apparatus.

References

[1] See e.g. J.E. Olsson, Proc. 5th Intern. Workshop on photon–photon collisions (Aachen, 1983), Springer Lecture Notes in Physics, Vol. 191 (Springer, Berlin, 1983) p. 45.
[2] Crystal Ball Collab., C. Edwards et al., Phys. Lett. 110B (1982) 82.
[3] CELLO Collab., H.J. Behrend et al., Phys. Lett. 114B (1982) 378; 125B (1983) 518(E).
[4] JADE Collab. (prelim.), Proc. 5th Intern. Workshop on photon–photon collisions (Aachen, 1983), Springer Lecture Notes in Physics, Vol. 191 (Springer, Berlin, 1983) p. 45.
[5] PLUTO Collab., Ch. Berger et al., DESY Report 84-074, Z. Phys. C, to be published.
[6] L. Criegee and G. Knies, Phys. Rep. 83 (1982) 153.
[7] H. Pilkuhn, Relativistic particle physics (Springer, Berlin, 1979).
[8] M.J. Corden et al., Nucl. Phys. B138 (1978) 235.
[9] Particle Data Group, Rev. Mod. Phys. 56 (1984) S1.
[10] V.M. Budnev et al., Phys. Rep. 15 (1975) 181.
[11] W.R. Frazer, J.R. Fulco and F.R. Halpern, Phys. Rev. 136 (1964) B1207.
[12] F. Selleri, Phys. Lett. 3 (1962) 76.
[13] See e.g. P. Grassberger and R. Kögerler, Nucl. Phys. B106 (1976) 451.
[14] G. Goldhaber et al., Phys. Rev. Lett. 15 (1965) 118.
[15] C.N. Yang, Phys. Rev. 77 (1950) 242.
[16] TASSO Collab., R. Brandelik et al., Z. Phys. C10 (1981) 117;
CELLO Collab., H.J. Behrend et al., Z. Phys. C23 (1984) 223;
PEP4/PEP9 Collab. (prelim.), submitted to the XXII Intern. Conf. on High energy physics (Leipzig, 1984).
[17] PLUTO Collab., Ch. Berger et al., Phys. Lett. 94B (1980) 254;
MARK II Collab., A. Roussarie et al., Phys. Lett. 105B (1981) 304;
J.R. Smith et al., SLAC-PUB-3205, to be published in Phys. Rev.;
DELCO Collab., A. Courau et al., Phys. Lett. 147B (1984) 227.
[18] TASSO Collab., M. Althoff et al., Phys. Lett. 121B (1983) 216.